

AIM and ELF bonding analyses of M–O and M–N (Metal= Ba, Y, Zr) in metal–complexes using DFT approach

Nor Ain Fathihah Abdullah¹, Sharizal Hasan¹ and Lee Sin Ang^{1*}

¹Faculty of Applied Sciences, Universiti Teknologi MARA, Perlis Branch, Arau Campus, 02600 Arau, Perlis, Malaysia.

Corresponding author: anglee631@uitm.edu.my

Received: 26 October 2020; Accepted: 10 December 2020; Published: 5 January 2021

ABSTRACT

The molecular interaction between the chelating agents of citric acid (CA), ethylenediaminetetraacetic acid (EDTA), and triethylenetetraamine (TETA) with metals (M = Ba, Y, and Zr) were studied using Density Functional Theory (DFT) method. This study aims to determine the type of bonding between M–O/N bonds in the CA/EDTA/TETA– complexes. In this study, each metal was attached at strategic positions of chelating agents and was optimized at B3LYP/6-31G* and UGBS level of theory. The M–O bonds were characterized based on Atoms-in-molecules (AIM) and Electron Localization Function (ELF) in the topological analysis. In AIM analysis, the total electron energy density at the bond critical point (BCP) of the M–O/N bonds are used to estimate the interaction involved. The low values of $\rho(r)$ and positive values of $\nabla^2\rho(r)$ indicates that ionic character exists in the M–O/N bonds. In ELF color-filled map, the blue shaded region between M–O/N atom acts as an indicator for the existence of the ionic interaction. Both AIM and ELF results confirm the existence of ionic bonding between M–O/N bonds, with values of $\rho(r)$ and $\nabla^2\rho(r)$ ranging from 0.02 to 0.12 au and 0.09 to 0.5 au respectively. Further analysis on charge distribution at M–O/N bonds show that the opposite charge between Ba, Y, and Zr with O/N assured the M– O/N ionic bonding interactions.

Keywords: *Density functional theory, metals, bonding, atom-in-molecules, bond critical point, electron localization functions*

INTRODUCTION

In past years, chelating agents such as CA, EDTA, and TETA are tremendously used as a chelator to trap metal in various fields such as the cleaning industry, medical treatment, food industry, to name a few. These chelating agents possessed lone pair electron that can bind with metal to form metal-complexes. Recently, CA, EDTA, and TETA have been subjected by researchers in the initial step of the formation of metal-complexes in producing ceramic materials [1-3]. As reported in [3], the presence of these chelating agents in the initial step produces better results in the formation of metal oxide. Different chelating agents give different strengths during the chelation process. Hence, these initial steps are vital to obtaining stable metal-complexes for use in the subsequent process. However, the understanding of chemical bonding involved in the metal-complexes at the molecular level is still ambiguous when involving large metals such as barium (Ba), yttrium (Y), and zirconium (Zr).

The chemical bonds are of utmost importance in understanding the chemical phenomena. Chemical bonds are the attraction between two or more atoms, which involved the sharing or transfer of electrons (covalent/ionic) [4]. The different type of chemical bonds gives different chemical and physical properties of the compound. There are numerous theoretical studies on the analysis of chemical bonding [5-9]. Atom-in-molecules (AIM) [10] and Electron Localization Function (ELF) [11] are among the tools that have been used to determine the chemical bonding in a compound. Both AIM and ELF are approaches to electron density analysis. These analyses can be used, for example, to elucidate the bonding of the removal or adsorption of chemical compounds [12,13].

In this study, we performed quantum mechanical calculations on metal-complexes at the microscopic level. To determine the chemical bonding nature of M–O, and M–N bonds in metal-complexes, the AIM and ELF analysis have been carried out on the most stable configurations of the complexes considered. This analysis would help chemists or physicists to get a better understanding of the chemical bonds in the metal-complexes at the molecular level. The binding energies of the configurations and the related discussion have been previously reported [14].

EXPERIMENTAL

Theoretical Section

All molecular geometries were fully optimized at DFT by using hybrid functional of Becke–3-parameter (B3) [15] and Lee–Yang–Parr (LYP) [16], also known as B3LYP, together with 6–31G* and UGBS basis sets. These two basis sets are included because of the unavailability of the 6–31G* to the metals, and UGBS is a capable basis set to model the wave function of the metals. To

imitate the pH condition, CA is deprotonated by the removal of three hydrogen atoms. Each metal (Ba, Y, and Zr) was initially attached to the strategic position of CA. All calculations are carried out in the Gaussian09 suite of programs [17]. The AIM and ELF analysis are performed using Multiwfn [18] software. AIM can identify the type of chemical bonding by considering selected properties at some critical points. The electron density, $\rho(r)$ and Laplacian electron density, $\nabla^2\rho(r)$ at BCP between two pair atoms often used as a descriptor to understand chemical bonding involved. The ELF is a probability of finding an electron in regions of space at a given point by analyzing the function in the form of:

$$ELF(r) = \frac{1}{1 + \left(\frac{D(r)}{D_o(r)}\right)^2}, \quad (1)$$

Where

$$D(r) = \frac{1}{2} \sum_{i=1}^N \nabla \varphi_i(r)^2 - \frac{1}{8} \frac{|\nabla \rho(r)|^2}{\rho(r)}, \quad (2)$$

$$D_o(r) = \frac{3}{10} (3\pi^2)^{\frac{2}{3}} \rho(r)^{\frac{5}{3}}, \quad (3)$$

$$\rho(r) = \sum_{i=1}^N |\varphi_i(r)|^2. \quad (4)$$

The summation of i is done for all N φ_i molecular orbitals; $D(\mathbf{r})$ is indicated as the excess kinetic energy density caused by Pauli repulsion, while $D_o(\mathbf{r})$ is considered as Thomas-Fermi kinetic energy density for homogeneous electron gas; $\rho(\mathbf{r})$ is the electron density. ELF introduced by Becke and Edgecombe [11], describes the bonding takes place between two pair of atoms. The unit-less values of ELF are restricted from 0 to 1.

RESULTS AND DISCUSSION

The topological analysis based on electron density were analyzed from the wave function obtained at B3LYP/6-31G* level of theory. Results from AIM analysis of electron density for metal-complexes systems revealed the BCP in M-CA/EDTA/TETA complexes. BCP is the point between two adjacent atoms, which defines a bond between the atoms. The positions of BCP (orange dots) in the M-CA/EDTA/TETA complexes system were portrayed in Figures 1-2. It can be noticed from Figure 1 that the small orange dots indicate BCP exists between M-O/N bonds nearby. This shows that the electron density is practically built-up between these M-O/N bonds.

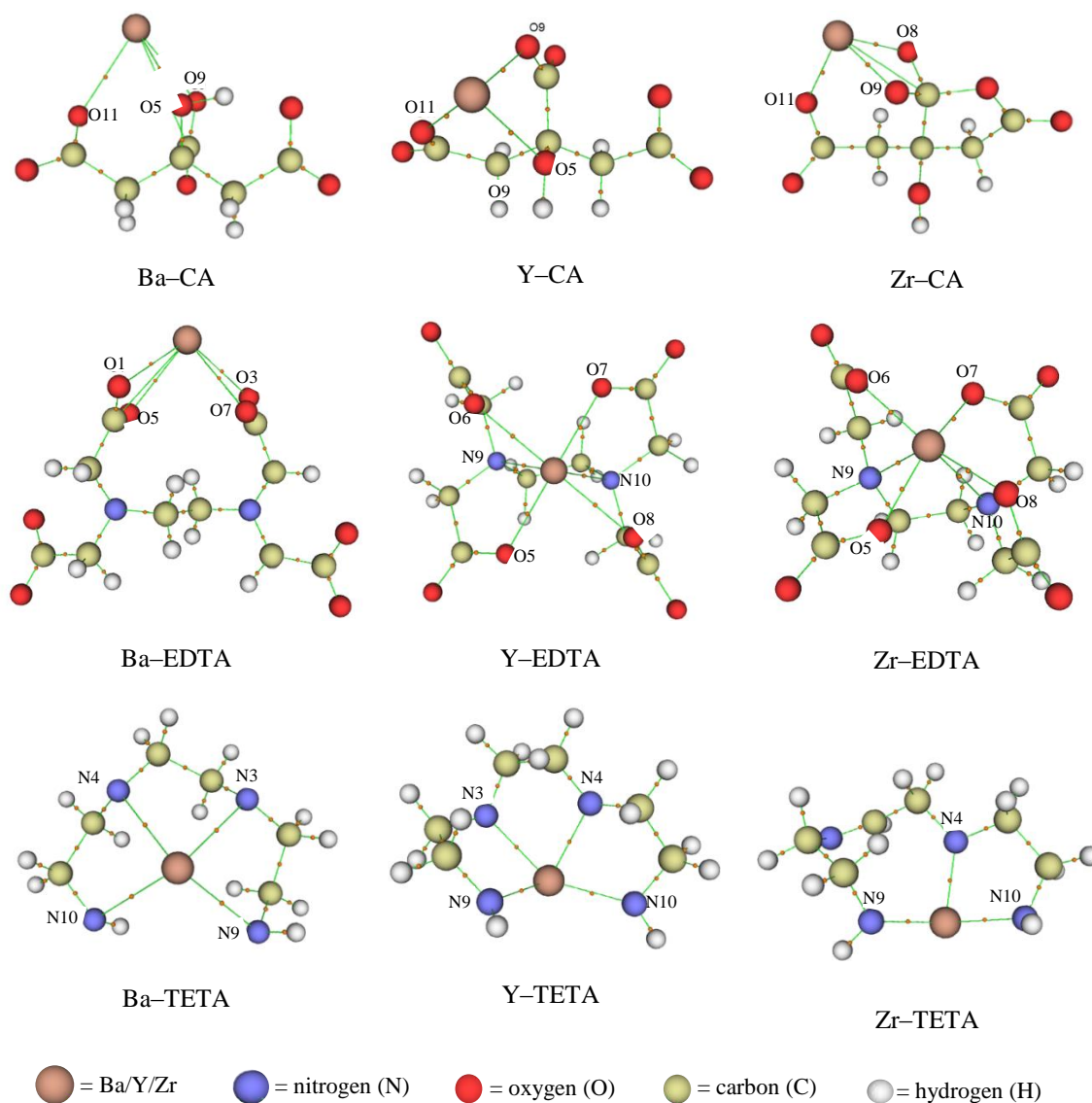


Figure 1: Positions of the BCP (orange dot) critical points in metal-CA/EDTA/TETA complexes

The parameters of BCP can be related to the interatomic interaction such as ionic, covalent, or van der Waals interaction [10,19]. To give a deep understanding of the interactive nature between M-O/N in these metal complexes, the BCP at M-O, and M-N bond are characterized by electron density ($\rho(r)$) and Laplacian electron density ($\nabla^2\rho(r)$). Value of electron density ($\rho(r)$) and the sign of Laplacian of electron density ($\nabla^2\rho(r)$) are significant in determining the type of bonding.

The large value of $\rho(r)$ indicates the strong covalent bonding [20,21], while the Laplacian elucidates the accumulation ($\nabla^2\rho(r) < 0$) and depletion ($\nabla^2\rho(r) > 0$) of charge [22]. The corresponding properties of the BCP at M–O, and M–N bonds for metal–CA/EDTA/TETA complexes were tabulated in Tables 1, 2, and 3 respectively.

In general, all the values of $\rho(r)$ obtained for all metal–complexes at M–O/N bonds are low, in the range of ~ 0.02 to 0.12 au (as shown in Tables 1, 2, 3). The $\nabla^2\rho(r)$ observed for all metal–complexes are found to exhibit a positive value in the range of ~ 0.05 to 0.50 au. According to [23], the low value of $\rho(r)$ and the positive value of $\nabla^2\rho(r)$ represents a non–covalent character. Vice versa, the large values of $\rho(r)$ (~ 0.5) and negative $\nabla^2\rho(r)$ (around -0.9) at BCP between C–N atoms indicates the involvement of covalent interactions [20]. It also reported by other work [10], that the high values of $\rho(r) > 10^{-1}$ is referred to as the covalent system while the small values of $\rho(r) \approx 10^{-2}$ is referred to as the ionic system. Hence, this is a clear indication that the interaction involved is non–covalent. Based on these reports [10, 20-23], it can be concluded that the corresponding bond between M–O/N in this work is non–covalent bonding.

The electron localization function (ELF) value of BCP at M–O/N bond also is identified quantitatively by AIM (as tabulated in Tables 1 to 3). ELF is a probability of finding an associated electron pair in the space at a given point [11]. ELF has been widely used to study the chemical bonding and atomic shell structure in a variety of systems [24-26]. Becke and Edgecombe [11] had restricted the value for ELF within a range of 0 to 1. The value close to 1 is interpreted as a perfect localization of electron while a value close to 0 is interpreted as delocalization of electron.

As shown in Table 1, the ELF values for Ba–O, Y–O, and Zr–O in metal–CA complex calculated by AIM are low (in the range of ~ 0.1 to 0.28). Similar results are obtained for M–O/N in metal–EDTA and metal–TETA complexes where the ELF values are ranging from 0.08 to 0.32 au. The low ELF value between two bonded atoms implies its ionic nature [7]. The values which are under ~ 3.5 are commonly considered as having the ionic character [6,20]. To establish the chemical bonding that takes place between M–O/N bonds, further analysis on ELF topological surface are determined and discussed in the next paragraph.

Table 1: Properties of selected BCP (M–O) for M–CA complexes

Bond (M–O)	Electron density, $\rho(r)$	Laplacian electron density, $\nabla^2\rho(r)$	ELF
Ba–O5	0.032	0.108	0.107
Ba–O9	0.039	0.138	0.123
Ba–O11	0.037	0.139	0.110
Y–O5	0.049	0.216	0.119

Y-O9	0.079	0.339	0.181
Y-O11	0.076	0.352	0.161
Zr-O8	0.114	0.416	0.267
Zr-O9	0.118	0.428	0.273
Zr-O11	0.110	0.486	0.215

Table 2: Properties of selected BCP (M-O/N) for M-EDTA complexes.

Bond (M-O/N)	Electron density, $\rho(r)$	Laplacian electron density, $\nabla^2\rho(r)$	ELF
Ba-O1	0.029	0.094	0.099
Ba-O3	0.029	0.097	0.101
Ba-O5	0.032	0.106	0.111
Ba-O7	0.031	0.103	0.108
Y-O5	0.059	0.266	0.135
Y-O6	0.056	0.251	0.130
Y-O7	0.059	0.266	0.135
Y-O8	0.056	0.250	0.130
Y-N9	0.041	0.137	0.146
Y-N10	0.041	0.137	0.147
Zr-O5	0.087	0.377	0.192
Zr-O6	0.083	0.360	0.182
Zr-O7	0.087	0.377	0.192
Zr-O8	0.083	0.360	0.182
Zr-N9	0.055	0.158	0.221
Zr-N10	0.055	0.158	0.221

Table 3: Properties of selected BCP (M–N) for M–TETA complexes.

Bond (M–O)	Electron density, $\rho(r)$	Laplacian electron density, $\nabla^2\rho(r)$	ELF
Ba–N3	0.040	0.106	0.178
Ba–N4	0.041	0.111	0.183
Ba–N9	0.040	0.104	0.182
Ba–N10	0.039	0.102	0.182
Y–N3	0.062	0.204	0.203
Y–N4	0.072	0.231	0.231
Y–N9	0.071	0.247	0.205
Y–N10	0.065	0.245	0.171
Zr–N4	0.108	0.337	0.282
Zr–N9	0.107	0.335	0.280
Zr–N10	0.102	0.278	0.315

Figure 2 shows the ELF color-filled map surface for metal–CA/EDTA/TETA complexes. In this analysis, the ELF topological surface is focussed on the region between metals (Ba, Y, and Zr) and oxygen or nitrogen atoms. The color range is from 0 (blue) to 1 (red). The red region elucidates the localization of electrons while the blue region (0) elucidates the delocalization of electrons. For all metal–complexes, the region between C–C atoms is shaded with orange color (refer Figure 2), which indicates that the electrons are localized. Hence, C–C bonds are covalent [24]. The red color on hydrogen (H) atoms implies a very high ELF value. In contrast, the region between metal Ba, Y, and Zr and oxygen or nitrogen are shaded with a blue color where electrons are delocalized, resulting in a low ELF value (close to 0). This blue region indicates that the involvement of ionic interaction between metals Ba, Y, Zr, and O atom [24]. The ELF color-filled map results correlate well with the ELF value calculated by AIM analysis (as tabulated in Tables 1 to 3).

This result also can be related to the decreasing charge of metal cations. Further analysis on charge distribution at M–O atoms shows that metal possessed a positive charge while oxygen possessed a negative charge. The original charge of metal Ba (+2), Y (+3), and Zr (+4) is decreased. The charge for metal and average charge for oxygen are as follow: Ba = +1.544, Y = +2.104, Zr = +2.672 and O = –0.4 to –0.7. Metal Ba, Y, and Zr possessed a positive charge due to the transfer of electrons while oxygen become negatively charged due to the gain of electrons. The decreasing charge of metal cations shows that the charge transfer occurs between M–O or M–N

bonds [27-28]. This is a clear indication that the transfer of charges occurs at M–O/N bond, thus assured the ionic interaction at M–O, and M–N bonds [29].

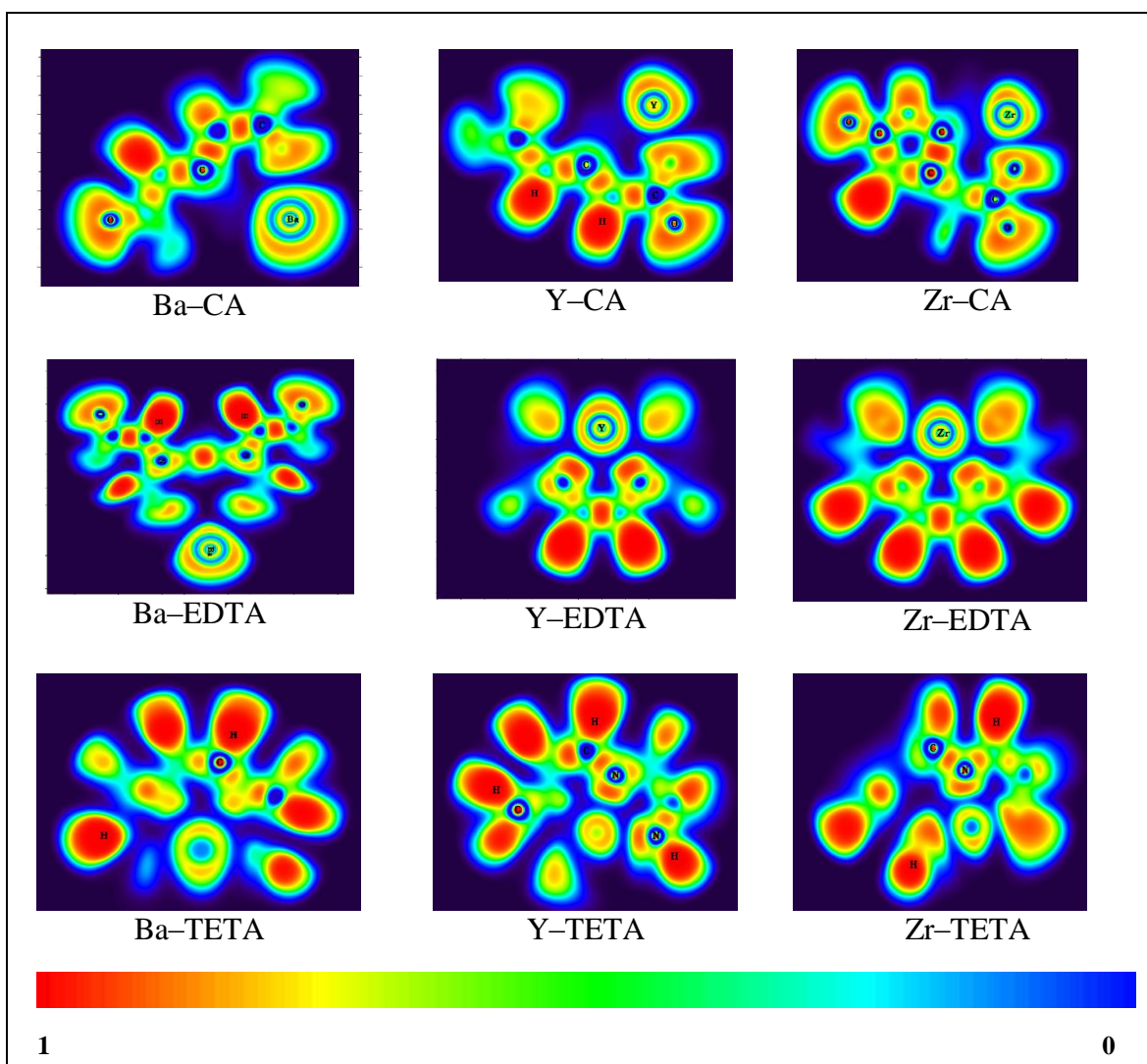


Figure 2: The ELF color-filled map of metal–CA/EDTA/TETA complexes

CONCLUSION

The bonding analysis has been carried out by using AIM and ELF topological analysis to understand chemical bonding takes place between M–O/N bonds in metal-complexes. The AIM

reveals the existence of a bond between metal Ba, Y, Zr, and oxygen/nitrogen atom via BCP. Based on the AIM analysis, the value of $\rho(r)$ and $\nabla^2\rho(r)$ obtained corroborates well with their ionic nature. For all metal-complexes, the low ELF value with the blue shaded region between Ba–O/N, Y–O/N, and Zr–O/N bonds in the ELF color-filled map elucidate the involvement of ionic interaction. Both AIM and ELF results confirming the existence of ionic bonding between M–O/N bonds with values of $\rho(r)$ and $\nabla^2\rho(r)$ ranging from 0.02 to 0.12 au and 0.09 to 0.50 au respectively. Further analysis on charge distribution at M–O/N bonds show that the opposite charge between Ba, Y, and Zr with O and the reduction of metal cations charge assured the M–O/N ionic bonding interactions. This study on the chemical bonding of metal-ligand complexes will be useful for providing a platform to understand the bonding nature of metal-oxygen and metal-nitrogen qualitatively and quantitatively at a molecular level.

ACKNOWLEDGMENTS

The authors would like to acknowledge the support of Universiti Teknologi MARA (UiTM) in providing the facilities and financial support for this research.

REFERENCES

- [1] Nafisah, O., Abdullah, N. A., & Hasan, S. (2014). Chelating agent role in synthesizing cerate-zirconate powder by a sol-gel method. In *Advanced Materials Research* (Vol. 896, pp. 112-115). Trans Tech Publications Ltd.
- [2] Abdullah, N. A., Osman, N., Hasan, S., & Nordin, R. M. (2012). The effect of various chelating agents on the thermal decomposition of cerate-zirconate ceramics powder. *APCBEE Procedia*, 3, 28-32.
- [3] Gao, D., & Guo, R. (2010). Yttrium-Doped Barium Zirconate Powders Synthesized by the Gel-Casting Method. *Journal of the American Ceramic Society*, 93(6), 1572-1575.
- [4] Frenking, G., & Froehlich, N. (2000). The nature of the bonding in transition-metal compounds. *Chemical reviews*, 100(2), 717-774.
- [5] Frenking, G., & Shaik, S. (Eds.). (2014). *The Chemical Bond: Chemical Bonding Across the Periodic Table* (Vol. 2). John Wiley & Sons.
- [6] Causa, M., D'Amore, M., Garzillo, C., Gentile, F., & Savin, A. (2013). The bond analysis techniques (ELF and maximum probability domains) application to a family of models relevant to bio-inorganic chemistry. In *Applications of density functional theory to biological and bioinorganic chemistry* (pp. 119-141). Springer, Berlin, Heidelberg.
- [7] Pan, S., Saha, R., & Chattaraj, P. K. (2015). Exploring the nature of silicon-noble gas bonds in H₃SiNgNSi and HSiNgNSi compounds (Ng= Xe, Rn). *International journal of molecular sciences*, 16(3), 6402-6418.

- [8] Kamaal, S., Usman, M., Afzal, M., Alarifi, A., Ali, A., Das, R., & Ahmad, M. (2021). A new copper (II)-based layered coordination polymer: Crystal structure, topology, QTAIM analysis, experimental and theoretical magnetic properties based on DFT combined with broken-symmetry formalism (BS-DFT). *Polyhedron*, 193, 114881.
- [9] Nguyen, M. N., Weidler, P. G., Schwaiger, R., & Schäfer, A. I. (2020). Interactions between carbon-based nanoparticles and steroid hormone micropollutants in water. *Journal of Hazardous Materials*, 122929.
- [10] Bader, R. F. W., & Nguyen-Dang, T. T. (1981). Quantum theory of atoms in molecules–Dalton revisited. In *Advances in Quantum Chemistry* (Vol. 14, pp. 63-124). Academic Press.
- [11] Becke, A. D., & Edgecombe, K. E. (1990). A simple measure of electron localization in atomic and molecular systems. *The Journal of chemical physics*, 92(9), 5397-5403.
- [12] Malek N. N. A., Yousif E., & Jawad A. H. (2020). Oil Optimization of Adsorption Parameters for Reactive Red 4 (RR4) Removal by Cross-linked Chitosan-Epichlorohydrin using Box-Behnken Design. *Science Letters*, 14(1), 83-95.
- [13] Nuzul M. I., & Abdul Karim S. K. (2020). Cr (VI) ions removal from aqueous solutions using carrot residues as an adsorbent. *Science Letters*, 13(2), 30-36.
- [14] Abdullah, N. A. F., & Ang, L. S. (2018). Binding Sites of Deprotonated Citric Acid and Ethylenediaminetetraacetic Acid in the Chelation with Ba²⁺, Y³⁺, and Zr⁴⁺ and Their Electronic Properties: a Density Functional Theory Study. *Acta Chimica Slovenica*, 65(1), 231-238.
- [15] Becke, A. D. (1988). Density-functional exchange-energy approximation with correct asymptotic behavior. *Physical review A*, 38(6), 3098.
- [16] Lee, C., Yang, W., & Parr, R. G. (1988). Development of the Colle-Salvetti correlation-energy formula into a functional of the electron density. *Physical review B*, 37(2), 785.
- [17] Frisch M. J., Trucks G. W., Schlegel H. B., Scuseria G. E., Robb M. A., Cheeseman J. R., Scalmani G., Barone V., Mennucci B., Petersson G.A., Nakatsuji H., Caricato M., Li X., Hratchian H.P., Izmaylov A.F., Bloino J., Zheng G., Sonnenberg J. L., Hada M., Ehara M., Toyota K., Fukuda R., Hasegawa J., Ishida M., Nakajima T., Honda Y., Kitao O., Nakai H., Vreven T., Montgomery J. A. Jr., Peralta J. E., Ogliaro F., Bearpark M., Heyd J. J., Brothers E., Kudin K. N., Staroverov V. N., Kobayashi R., Normand J., Raghavachari K., Rendell A., Burant J. C., Iyengar S. S., Tomasi J., Cossi M., Rega N., Millam M. J., Klene M., Knox J. E., Cross J. B., Bakken V., Adamo C., Jaramillo J., Gomperts R., Stratmann R. E., Yazyev O., Austin A. J., Cammi R., Pomelli C., Ochterski J. W., Martin R. L., Morokuma K., Zakrzewski V. G., Voth G. A., Salvador P., Dannenberg J. J., Dapprich S., Daniels A. D., Farkas Ö., Foresman J. B., Ortiz J. V., Cioslowski J., & Fox D. J., *Gaussian 09 Revision D.01*, Gaussian, Inc., Wallingford CT USA (2013).
- [18] Lu, T., & Chen, F. (2012). Multiwfn: a multifunctional wavefunction analyzer. *Journal of computational chemistry*, 33(5), 580-592.
- [19] Bianchi, R., Gervasio, G., & Marabello, D. (2000). Experimental electron density analysis of Mn₂(CO)₁₀: metal–metal and metal–Ligand bond characterization. *Inorganic Chemistry*, 39(11), 2360-2366.

- [20] Ryzhikov, M. R., Kozlova, S. G., & Gabuda, S. P. (2008). Strained bonds in [Re 4 Q 4 X 12] 4- cluster complexes (Q= S, Se, Te; X= F, CN-) according to AIM and ELF data. *Journal of Structural Chemistry*, 49(4), 587-594.
- [21] Khalili, B., & Rimaz, M. (2017). Does interaction between an amino acid anion and methylimidazolium cation lead to a nanostructured ion pairs of [Mim][AA] as an ionic liquid?. *Journal of Molecular Liquids*, 229, 267-277.
- [22] Stephen, A. D., Kumaradhas, P., & Pawar, R. B. (2011). Charge density distribution, electrostatic properties, and impact sensitivity of the high energetic molecule TNB: a theoretical charge density study. *Propellants, Explosives, Pyrotechnics*, 36(2), 168-174.
- [23] Soliman, S. M., Albering, J., & Abu-Youssef, M. A. (2017). Structural analyses of two new highly distorted octahedral copper (II) complexes with quinoline-type ligands; Hirshfeld, AIM and NBO studies. *Polyhedron*, 127, 36-50.
- [24] Chen, K., & Kamran, S. (2013). Bonding characteristics of tic and tin.
- [25] Burt, J. B., Gibbs, G. V., Cox, D. F., & Ross, N. L. (2006). ELF isosurface maps for the Al 2 SiO 5 polymorphs. *Physics and chemistry of minerals*, 33(2), 138-144.
- [26] Fuster, F., & Grabowski, S. J. (2011). Intramolecular hydrogen bonds: the QTAIM and ELF characteristics. *The Journal of Physical Chemistry A*, 115(35), 10078-10086.
- [27] Adeowo, F. Y., Honarparvar, B., & Skelton, A. A. (2016). The interaction of NOTA as a bifunctional chelator with competitive alkali metal ions: a DFT study. *RSC advances*, 6(83), 79485-79496.
- [28] Skelton, A. A., Agrawal, N., & Fried, J. R. (2015). Quantum mechanical calculations of the interactions between diazacrowns and the sodium cation: an insight into Na+ complexation in diazacrown-based synthetic ion channels. *RSC Advances*, 5(68), 55033-55047.
- [29] Coll, R. K., & Treagust, D. F. (2003). Investigation of secondary school, undergraduate, and graduate learners' mental models of ionic bonding. *Journal of Research in Science Teaching: The Official Journal of the National Association for Research in Science Teaching*, 40(5), 464-486.